[CANCER RESEARCH 61, 1486–1492, February 15, 2001]

Identification and Characterization of A-105972, an Antineoplastic Agent

Jinshyun R. Wu-Wong,[1] Jeffery D. Alder, Lisa Alder, David J. Burns, Edward K-H. Han, Bruce Credo, Stephen K. Tahir, Brian D. Dayton, Patricia J. Ewing, and William J. Chiou

Pharmaceutical Products Division, Abbott Laboratories, Abbott Park, Illinois 60064 [J. D. A., L. A., D. J. B., E. K-H. H., B. C., S. K. T., B. D. D., P. J. E., W. J. C.] and Santa Clara, California 95054 [J. R. W.]

ABSTRACT

A high-throughput screening assay was designed to select compounds that inhibit the growth of cultured mammalian cells. After screening more than 60,000 compounds, A-105972 was identified and selected for further testing. A-105972 is a small molecule that inhibits the growth of breast, central nervous system, colon, liver, lung, and prostate cancer cell lines, including multidrug-resistant cells. The cytotoxic IC_{50} values of A-105972 were between 20 and 200 nM, depending on the specific cell type. The potency of A-105972 is similar in cells expressing wild-type or mutant p53. A majority of cells treated with A-105972 were trapped in the G_2-M phases, suggesting that A-105972 inhibits the progression of the cell cycle. Using [^{3}H]A-105972, we found that A-105972 bound to purified tubulin. Unlabeled A-105972 competed with [^{3}H]A-105972 binding with an IC_{50} value of 3.6 μM. Colchicine partially inhibited [^{3}H]A-105972 binding with an IC_{50} value of ~90 μM, whereas paclitaxel and vinblastine had no significant effect. Tumor cells treated with A-105972 were observed to contain abnormal microtubule arrangement and apoptotic bodies. DNA ladder studies also indicated that A-105972 induced apoptosis. A-105972 caused a mobility shift of bcl-2 on SDS-PAGE, suggesting that A-105972 induced bcl-2 phosphorylation. A-105972 treatment increased the life span of mice inoculated with B16 melanoma, P388 leukemia, and Adriamycin-resistant P388. These results suggest that A-105972 is a small molecule that interacts with microtubules, arrests cells in G_2-M phases, and induces apoptosis in both multidrug resistance-negative and multidrug resistance-positive cancer cells. A-105972 and its analogues may be useful for treating cell proliferative disorders such as cancer.

INTRODUCTION

MDR[2] is either an innate or acquired resistance to a wide array of chemotherapeutic agents with diverse chemical structures and mechanisms of action. MDR is a serious problem, preventing the successful application of many otherwise efficacious therapeutics in the treatment of cancer (1). MDR is multifactorial, including the overexpression of P-glycoprotein (2), overexpression of MRP (3) and LRP (4), and mutation of the tumor suppressor p53 protein (5).

From a high-throughput screening assay based primarily on the inhibition of cell proliferation, A-105972 was identified as an antineoplastic agent that exhibits potency toward MDR+ cancer cells. We characterized A-105972 in both *in vitro* and *in vivo* assays. To synthesize more effective A-105972 analogues, the mechanism of action for the antineoplastic effect of A-105972 was investigated. In this report, we provide evidence that A-105972 is efficacious in inhibiting the growth of MDR+ cancer cells both *in vitro* and *in vivo* via interaction with microtubules. A-105972 likely binds to tubulins at a site that partially overlaps the colchicine binding site. A-105972 and its analogues are potentially useful in treating multidrug-resistant cancers.

MATERIALS AND METHODS

Materials. Paclitaxel, vinblastine, and colchicine were obtained from Sigma (St. Louis, MO). A-105972 and [^{3}H]A-105972 (20 Ci/mmol) were made at Abbott Laboratories. Other reagents were of analytical grade.

Cell Culture. All cell types used in this study were obtained from American Type Culture Collection (Manassas, VA). HT-1080, HCT-116, and HCT-15 were grown in DMEM (Life Technologies, Inc., Grand Island, NY) containing 10% (HT-1080 and HCT-116) or 20% (HCT-15) FBS (HyClone, Logan, UT). MCF-7 cells were cultured in Eagle's MEM containing nonessential amino acid, 1 mM sodium pyruvate, 10 μg/ml bovine insulin, and 10% FBS. HL-60 cells were maintained in suspension in RPMI 1640 containing 20% FBS. LNCaP cells were cultured in RPMI 1640 containing 10% FBS. PC-3 cells were cultured in Ham's F12K containing 7% FBS. All cells were cultured at 37°C in moisturized air containing 5% CO_2. Cell viability was examined by the trypan blue exclusion method. The cell lines used in this report are listed in Table 1.

Cell Proliferation. Cells in 48- or 96-well plates in growth medium were treated with A-105972 at different concentrations for 48 h. Cells were trypsinized, and the number of cells in each well was determined using a Coulter counter.

***In Vivo* Evaluation of A-105972.** Mice were obtained from Harlan Sprague Dawley (Indianapolis, IN). For efficacy evaluations, female BALB/c × DBA/2Fl (CD2Fl beige, hereafter referred to as CDF1) and C57BL/6 × DBA/2Fl (B6D2F1/Hsd black, hereafter referred to as BDF1) mice were housed 10 animals/cage on bedding and given free access to food and water. P388 tumor cells were harvested from donor ascites fluid, diluted approximately 20-fold, and injected i.p. at 10^6 cells/mouse into CDFl mice. B16 tumor cells were prepared by homogenizing a tumor in medium at a 1:20 ratio (w:v), and 0.5 ml of the cell suspension was injected i.p. into BDF1 mice. All drugs were delivered i.p. against i.p. tumors. A-105972 was diluted with sterile injectable water (Abbott Laboratories, North Chicago, IL) to yield appropriate concentrations, and 0.5 ml was administered i.p. A-l05972 was soluble at 3 mg/ml (yielding the 50 mg/kg dosage). The first dose was administered 1 day after tumor inoculation. Against P388 and P388ADR leukemic tumors, A-l05972 was administered once daily, for 5 consecutive days. Against B16, A-105972 was administered once daily for 9 consecutive days. Drug efficacy against i.p. tumors was based on the percentage increase in the life span of treated *versus* untreated mice. Dosages that caused greater than 20% mortality were classified as toxic and were not presented in efficacy data. The maximum tolerated dose was determined as the highest dose that produced <20% mortality.p

Flow Cytometry and Cell Cycle Analysis. Cells in 10-cm^2 Petri dishes in growth media were treated with A-105972. Cells were trypsinized, pelleted, and stained with 1 ml of staining solution containing 0.3 g/ml PEG 8000, 0.05 mg/ml propidium iodide, 0.025 mg/ml RNase, 0.1% Triton X-100, and 4 mM sodium citrate (pH 7.8) for 20 min at 37°C. After incubation, another milliliter of staining solution containing 0.3 g/ml PEG 8000, 0.05 mg/ml propidium iodide, 0.1% Triton X-100, and 400 mM NaCl (pH 7.2) was added, and the mixture was incubated at 4°C in darkness for more than 1 h. The cells were analyzed using a flow cytometer.

[^{3}H]A-105972 Binding to Purified Tubulin. BioSpin6 columns (Bio-Rad, Hercules, CA) were equilibrated in assay buffer [100 mM 2-[*N*-morpholino]ethanesulfonic acid (pH 6.9) and 0.5 mM $MgCl_2$] and centrifuged at 1100 × *g* for 2 min right before use. Purified bovine tubulin (50 μg; ICN, Costa Mesa, CA) was incubated with [^{3}H]A-105972 (final concentration, 30 nM or as indicated) in 200 μl of assay buffer in the presence of 100 μM test

Received 3/31/00; accepted 12/11/00.

The costs of publication of this article were defrayed in part by the payment of page charges. This article must therefore be hereby marked *advertisement* in accordance with 18 U.S.C. Section 1734 solely to indicate this fact.

[1] To whom requests for reprints should be addressed, at Abbott Laboratories, 5440 Patrick Henry Drive, Santa Clara, CA 95054. Phone: (408) 567-3298; Fax: (408) 567-3412; E-mail: ruth.r.wuwong@abbott.com.

[2] The abbreviations used are: MDR, multidrug resistance; MRP, MDR-associated protein; LRP, lung resistance protein; MAP, microtubule-associated protein; FBS, fetal bovine serum; EM, electron microscopy; PIPES, piperazine-*N*,*N*′-bis[2-ethanesulfonic acid]; NCI, National Cancer Institute; SPA, scintillation proximity assay; PBS-T, PBS containing 0.1% Tween 20; GI_{50}, concentration causing 50% growth inhibition.

Table 1 *The effect of A-105972 on the proliferation of cancer cell lines*

Name	Type	A-105972 IC_{50} (nM)	P-glycoprotein expression[a]
A549	Human lung carcinoma	3.0	Negative
COLO-205	Human colon cancer	158	+
HCT-15	Human colon cancer	100	+++++
HL-60	Human leukemia	17	Negative
HS-578T	Human breast cancer	90	NK
HT-29	Human colon cancer	8	Negative
HT-1080	Human fibrosarcoma	46	NK
LNCaP	Human prostate cancer	6	NK
MCF-7	Human breast cancer	15	Negative
MDA-468	Human breast carcinoma	100	NK
NCI-H226	Human lung cancer	96	+++
NCI-H460	Human lung cancer	48	Negative
PC-3	Human prostate cancer	51	NK

[a] +, positive; NK, not known.

agents (or as indicated) for 20 min at room temperature. After incubation, 80-μl aliquots from each sample were applied to the BioSpin6 column and centrifuged at 1100 $\times$ *g* for another 2 min. The eluent was collected for radioactivity determination. The radioactivity in each sample before the elution was also determined to calculate the percentage of radioactivity bound.

Alternatively, a SPA-based assay was used (Amersham, Bucks, United Kingdom). Coupling of antibodies to the SPA beads was carried out according to the manufacturer's instructions (Amersham). Briefly, SPA beads (0.1 g) were incubated with a rabbit-derived antitubulin polyclonal antibody (20-fold dilution; Sigma) in 6 ml of assay buffer [100 mM 2-[*N*-morpholino]ethanesulfonic acid (pH 7.4), 1 mM EGTA, 0.1 mM phenylmethylsulfonyl fluoride, and 0.5 mM $MgCl_2$] for more than 1 h at room temperature in the darkness. To block nonspecific binding sites, BSA (40 mg) was added, and the mixture was incubated for 10 min. Afterward, purified tubulin (2.4 mg) in 4 ml of assay buffer was added, and the mixture was incubated at room temperature for another 2 h. For binding studies, [^{3}H]A-105972 (10 μl of 0.6 μM) was incubated with 200 μl of SPA beads coupled with tubulin in the presence of test agents for 30 min at room temperature before counting. The SPA bead method offers the advantage that no additional step is needed to separate bound from unbound ligands. A more detailed description of the SPA technology was reported previously by us on a SPA-based receptor binding assay (6).

Assay of Microtubule Assembly. Bovine brain tubulin proteins containing MAPs were isolated according to a previously published procedure (7). Microtubules were reconstituted *in vitro* using either purified bovine tubulin without MAPs (ICN) or MAP-rich tubulin proteins prepared in house. Tubulin (3 mg/ml, final concentration) in 100 μl of buffer containing 80 mM PIPES (pH 6.9), 1 mM $MgCl_2$, 1 mM EGTA, 1 mM GTP, and 30% glycerol was placed in a 96-well microtiter plate in the presence or absence of test agents. The increase of absorbance was monitored at 350 nm in a SpectraMax 340 Microplate Reader at 37°C and recorded every 30 s for 30 min.

Acquisition and Analysis of EM Data. For EM studies, tubulins (3 mg/ml) with MAPs were incubated with test agents in assay buffer [80 mM PIPES (pH 6.9), 1 mM $MgCl_2$, and 1 mM EDTA] containing 30% glycerol and 1 mM GTP for 30 min at 37°C. Samples were fixed by dilution (1:20–1:50 fold) into assay buffer containing 30% glycerol and 0.5% glutaraldehyde at 35°C, and then 10 μl of each sample were spotted onto Formavar-coated grids and stained with uranyl acetate for 30 s. Electron micrographs were obtained using a Philips CM-12 transmission electron microscope with an accelerating voltage of 100 kV.

Immunocytostaining for Tubulin and Confocal Microscopy. Cells grown in two-chamber slides were treated with A-105972 at 10 μM for 24 h. Cells were washed with PBS for 30 s, fixed with a fixing solution (0.1% glutaldehyde, 2% formalin, 80 mM PIPES, 5 mM EGTA, 1 mM $MgCl_2$, and 0.5% Triton X-100) for 7 min, washed again with PBS for 5 min, placed in methanol at −20°C for 4 min, and then placed in acetone at −20°C for 2 min. The slides were rinsed with PBS plus 0.2% BSA three times and incubated with PBS plus 10% FBS for 1 h at room temperature. The slides were then incubated with an antitubulin antiserum derived from rabbits (Santa Cruz Biotechnology, Santa Cruz, CA) in PBS with 0.2% BSA for 1 h at 37°C. After incubation, slides were rinsed with PBS containing 0.2% BSA for three times and then incubated with a FITC-conjugated antirabbit antibody (Santa Cruz Biotechnology) for 1 h at 37°C, followed by another three rinses with PBS containing 0.2% BSA. To stain nuclei, slides were incubated with propidium iodide (1 mg/ml) for 20 min at room temperature and washed again with PBS containing 0.2% BSA. The slides were mounted and photographed with a confocal microscope linked to an image analyzer.

Apoptosis Studies. Cells were washed once with cold PBS, dissolved in lysis buffer (10 mM Tris, 10 mM EDTA, and 0.5% Triton X-100), and then incubated for 10 min at 4°C. Samples were spun at 16,000 rpm for 20 min. The supernatants were collected and then incubated with RNase (0.4 mg/ml) and proteinase K (0.4 mg/ml) for 1 h at 37°C. Fragmented DNAs were precipitated with NaCl (1 M) and isopropanol (50% final concentration) for 16 h at −20°C, and analyzed by electrophoresis on a 1.5% agarose gel.

SDS-PAGE and Western Blot Analysis. Cells in 10-cm^2 Petri dishes pretreated with or without test agents were solubilized in 600 μl of 10 mM Tris (pH 7.4), 5 mM EDTA, and 1% Triton X-100 for 20 min at 4°C, and the protein content in each sample was determined by the Bio-Rad dye-binding protein assay. Samples (120 μg/sample) were resolved by SDS-PAGE using a 12% gel (Novex, San Diego, CA), and proteins were electrophoretically transferred to nitrocellulose paper for Western blotting. The nitrocellulose paper was blotted for 1 h at 25°C with 5% nonfat dry milk in PBS-T and then incubated with an anti-bcl-2 antibody derived from mice (Santa Cruz Biotechnology) in PBS-T for 1 h at 25°C. The paper was washed with PBS-T and incubated with a horseradish peroxidase-labeled antimouse antibody for 1 h at 25°C. The paper was then incubated with detection reagent containing luminol in an alkaline buffer. The specific bands were visualized by exposing the paper to blue light-sensitive autoradiography films.

RESULTS

Cytotoxicity. A-105972 was identified from a high-throughput screening assay based on inhibition of cell proliferation. Fig. 1*A* shows the structure of A-105972, 4-[4-acetyl-4,5-dihydro-5-(3,4,5-trimethoxyphenyl)-1,3,4-oxadiazol-2-yl]-2-methylbenzeneamine.

The potency of A-105972 was determined in various cancer cell lines including human lung, colon, breast, and prostate cancer cells. Fig. 1*B* shows a typical result from the cytotoxicity study. The IC_{50} values for HL-60, HT-1080, and MCF-7 cells were 17, 46, and 15 nM, respectively. Table 1 lists the IC_{50} values of A-105972 tested in a

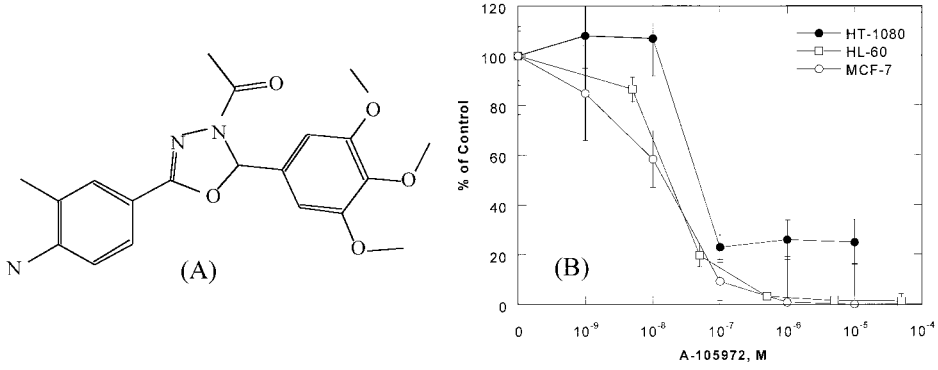

Fig. 1. A-105972 inhibited the proliferation of three cancer cell lines. *A*, the structure of A-105972. *B*, inhibition of cell proliferation. Cells in 48-well plates in growth medium were treated with A-105972 at different concentrations for 48 h. Cells were trypsinized, and the number of cells in each well was determined using a Coulter counter. To calculate the inhibition of growth, the number of cells at time 0 was first subtracted. The adjusted cell number was calculated as a percentage of the control, which was the number of cells in wells without the addition of A-105972. Each value represents the mean ± SD of three determinations.

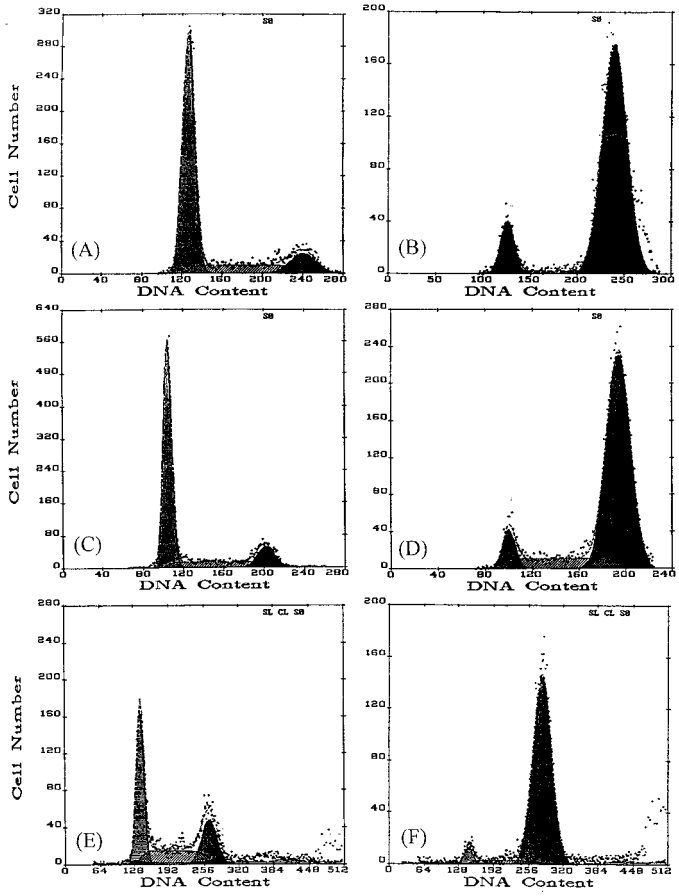

Fig. 2. A-105972 blocked the cell cycle at the G_2-M phase. Cells in 24-well plates in growth medium were treated with 1 μM A-105972 for 24 h. The DNA content of the cells was analyzed by a flow cytometer as described in "Materials and Methods." *A* and *B*, HCT-116; *C* and *D*, LNCaP; *E* and *F*, PC-3. *A*, *C*, and *E*, no treatment. *B*, *D*, and *F*, treatment with A-105972.

variety of cancer cell lines. The IC_{50} values of A-105972 were in the range of 20–200 nM, depending on the cell lines.

Effect of A-105972 on the Cell Cycle. The effect of A-105972 on cell cycle progression was examined in the aforementioned cancer cells. Fig. 2 shows typical results from treatment of HCT-116, LNCaP, and PC-3 cells with A-105972 at 1 μM for 24 h. It is evident that A-105972 treatment resulted in the accumulation of cells in G_2-M phase, suggesting that A-105972 blocked the cell cycle at the G_2-M phase.

Efficacy of A-105972 in Animal Tumor Models. A-105972, administered once daily for 9 consecutive days (days 1–9 after inoculation) produced a significant delay in death due to B16 ascites tumor (Fig. 3*A*). The effect was dose dependent and clinically significant for the 25 and 50 mg/kg dosages. At 50 mg/kg, A-105972 delayed death by approximately 8 days compared with controls. As a comparison, the positive control group of animals that received Adriamycin at 1, 2, and 4 mg/kg exhibited a >37-day delay in death. The plasma half-life of A-105972 was ~30 min in BDF1 mice (data not shown), which might account for the inferior efficacy of A-105972 in comparison with Adriamycin. In Fig. 3*B*, CDF1 mice were inoculated with P388 leukemic tumor cells and treated with vincristine or A-105972. At 25 mg/kg, A-105972 delayed death by approximately 5 days compared with controls. As a comparison, vincristine delayed death by 8 days. Fig. 3*C* shows the study in which P388/ADR (Adriamycin-resistant P388) cells were used. In this model, A-105972 at 25 mg/ml delayed death by approximately 3 days compared with controls. As a comparison, the vincristine-treated group did not demonstrate efficacy and exhibited a shorter life span, possibly due to the toxicity of the drug. These data suggest that A-105972 is efficacious *in vivo*.

A-105972 Evaluated in the NCI's 60 Human Cancer Cell Lines. A-105972 was evaluated by the NCI in a panel of 60 human cancer cell lines (8, 9). A-105972 exhibited a significant growth inhibition efficacy in most cancer cell lines, with the exception of two ovarian cancer cell lines, OVCAR-4 and OVCAR-5, and one renal cancer cell line, TK-10 (data not shown). The log GI_{50} values of A-105972 for the 60 cell lines range from −4.0 in TK-10 (renal cancer) to −8.0 in MALME-3 M (melanoma), with more than 90% of the values in the range of −6.5 to −7.5. The mean log GI_{50} was −7.16, which was equivalent to a GI_{50} of 69 nM. The COMPARE analysis of the mean GI_{50} graph revealed that A-105972 exhibited correlation coefficients of >0.6 with tubulin-interacting agents such as vinblastine, suggesting that A-105972 might act via a similar mechanism (data not shown).

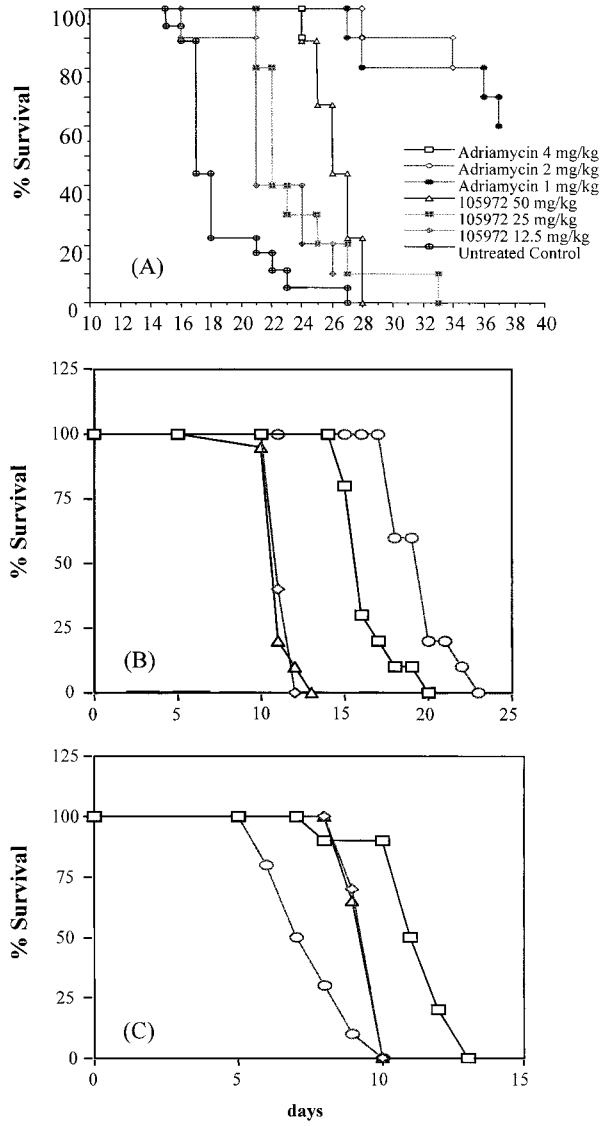

Fig. 3. A-105972 increased the life span of mice inoculated with cancer cells. *A*, B16 tumor cells were injected i.p. into BDF1 mice. A-105972 and Adriamycin were administered once daily (1 day after tumor cell inoculation) for 9 consecutive days. *B*, CDF1 mice were inoculated with P388. A-l05972 and vincristine were administered once daily for 5 consecutive days. C, same as in *B* except that P388/ADR leukemic tumor cells were used. *B* and *C*: △, untreated mice; ○, mice treated with vincristine (0.5 mg/kg); ◇, mice treated with A-105972 (5 mg/kg); □, mice treated with A-105972 (25 mg/kg).

A striking feature of A-105972 from the NCI analysis is the efficacy of the compound against the proliferation of MDR-1-overexpressing cell lines. For example, when the potency (GI_{50} values) of A-105972 or paclitaxel on inhibiting cell proliferation was plotted against the expression level of MDR-1 in the 60 cancer cell lines, the potency of paclitaxel was inversely proportional to the level of MDR-1, whereas the potency of A-105972 was completely independent of the MDR-1 level (data not shown). A similar analysis was done for MRP and LRP. The potency of A-105972 was independent of the levels of MRP and LRP. Furthermore, the potency of A-105972 was independent of the p53 status (data not shown).

These results suggest that A-105972 is effective in inhibiting MDR+ cells with mutated p53 and may interact with microtubules.

Binding of A-105972 to Purified Tubulin. We then synthesized tritium-labeled A-105972 and conducted binding studies using purified tubulins. Fig. 4*A* shows that [^{3}H]A-105972 binding to purified tubulin was inhibited by unlabeled A-105972 in a dose-dependent manner with an IC_{50} of 3.6 μM. The same study was repeated using both the BioSpin6 column and SPA bead assays, and similar results were obtained. From five independent SPA experiments, the K_i (or K_d) value for A-105972 was calculated to be 2.8 $\pm$ 2.0 μM (mean $\pm$ SD). Fig. 4*B* shows that, using the BioSpin6 column assay, the unlabeled A-105972 at 100 μM inhibited the binding of [^{3}H]A-105972 by >95%. Colchicine at 100 μM inhibited the binding by ~60%, whereas paclitaxel and vinblastine at 100 μM did not have a significant effect. Colchicine, albeit less potent than A-105972, also inhibited [^{3}H]A-105972 binding to purified tubulin in a dose-dependent manner with an IC_{50} at ~90 μM in the BioSpin6 column assay method (Fig. 4*C*). These data suggest that A-105972 likely binds to a site that is not identical to but partially overlaps with the colchicine binding site.

Microtubule Assembly Studies. The effect of A-105972 on microtubule polymerization was examined in an *in vitro* assay. First, microtubules were reconstituted *in vitro* using purified tubulin proteins lacking MAPs. The assembly of microtubules was detected by an increase in absorbance at 350 nm. Fig. 5*A* shows that in the control sample without addition of any test agent, the absorbance at 350 nm increased following time. The rate of increase was initially slow but accelerated at ~2 min after the initiation of the reaction. The increase in the $A_{350\ nm}$ reached a plateau at ~8 min. In the presence of 100 μM A-105972, polymerization was completely inhibited throughout the reaction. As a comparison, in the presence of paclitaxel, the absorbance at 350 nm increased at a constant rate from the very beginning and reached a plateau at 5 min.

Fig. 5*B* shows the result of microtubule assembly *in vitro* using MAP-rich tubulin. In the control sample without the addition of any test agent, the absorbance at 350 nm again increased following time. The rate of increase was initially slow, accelerated at ~5 min after the initiation of the reaction, and then reached a constant rate at ~10 min. In the presence of 100 μM colchicine, polymerization was completely inhibited in the first 7 min of the reaction. Turbidity started to increase at 7 min, but the rate of microtubule assembly was lower than that in the control sample. In the presence of A-105972, there was a slow increase in turbidity in the first 10 min. At 10 min after the initiation of the reaction, the rate of microtubule assembly increased to the same extent as that in the control sample. The results suggest that A-105972 inhibited microtubule assembly *in vitro*.

In Fig. 6, the effect of A-105972 on microtubule assembly was compared with that of paclitaxel and vinblastine in EM studies. In the study, tubulin polymerization was initiated by the addition of tubulins. In the presence of 10 μM paclitaxel, long microtubules that appeared rigid and ribbon-like were formed, suggesting that paclitaxel stabilized microtubules (Refs. 10 and 11; Fig. 6*A*). In the presence of 100 μM vinblastine, structures like spiral protofilaments, but not microtubules, were observed, consistent with the previous observation that vinblastine disrupts microtubule assembly (Refs. 10 and 11; Fig. 6*B*). As a comparison, in the presence of 100 μM A-105972, short fragments of microtubules were present (Fig. 6*C*).

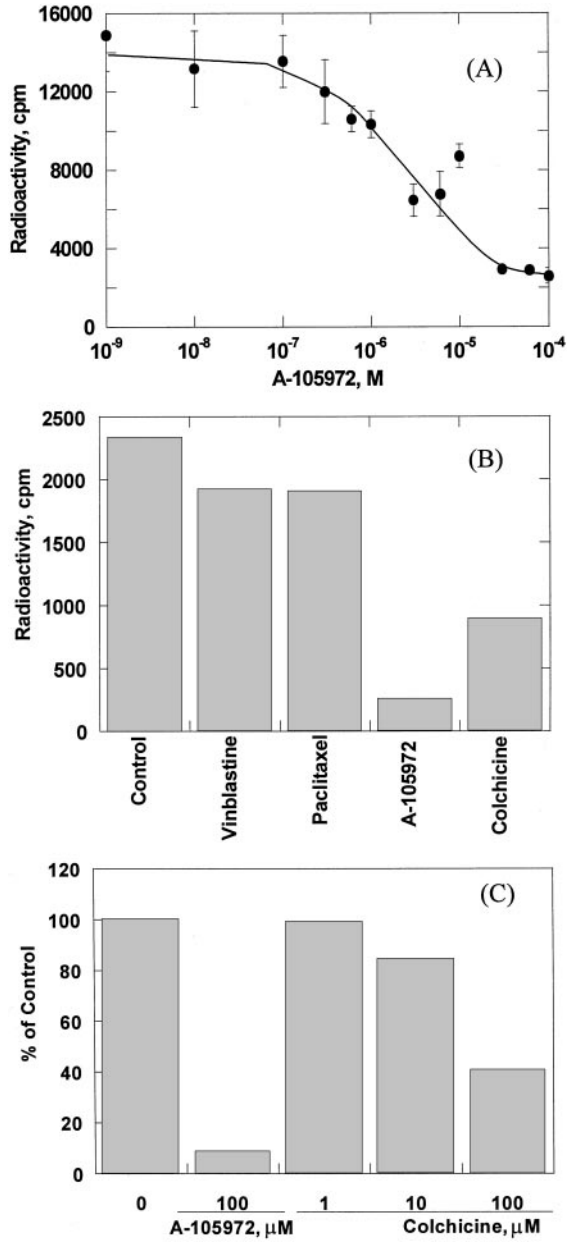

Fig. 4. A-105972 bound to tubulin. *A*, [^{3}H]A-105972 (150 nM, final concentration) was incubated with 200 μl of SPA beads coupled with purified tubulin in the presence of increasing concentrations of A-105972 for 30 min at room temperature before counting as described in "Materials and Methods." Each value represents the mean $\pm$ SD of three determinations. *B*, purified tubulin (50 μg) was incubated with [^{3}H]A-105972 (30 nM, final concentration) in 200 μl of assay buffer in the presence of 100 μM test agents for 20 min at room temperature. After incubation, free [^{3}H]A-105972 was separated from tubulin-bound [^{3}H]A-105972 using the BioSpin6 column as described in "Materials and Methods." Each value represents the mean of two determinations. *Control*, no addition of test agents. *C*, same as in *B*, except that increasing concentrations of colchicine and 100 μM A-105972 were tested against control (no addition of test agents). The radioactivity of each sample was calculated as a percentage of the control. Each value represents the mean of two determinations.

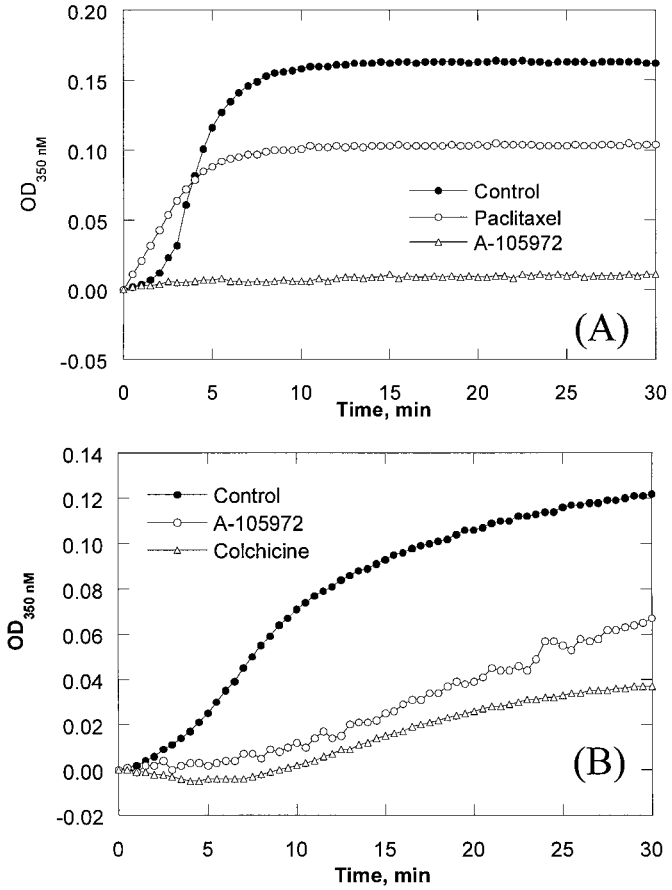

Fig. 5. Effects of A-105972 on microtubule assembly. Purified tubulin proteins without MAPs (*A*) or MAP-rich tubulin proteins (*B*) in a PIPES buffer containing 1 mM GTP were incubated at 37°C in the absence (*Control*) or presence of A-105972 (100 μM), colchicine (100 μM), or paclitaxel (100 μM) for 30 min. Polymerization was initiated by the addition of tubulin. Turbidity was measured at 350 nm.

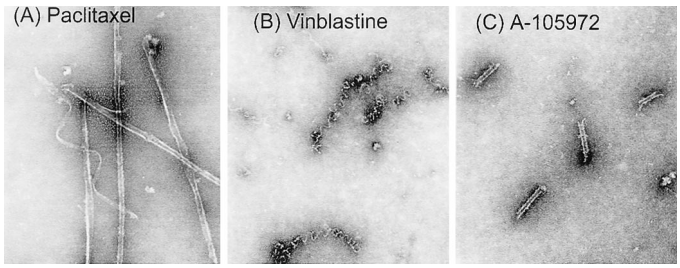

Fig. 6. A-105972 treatment resulted in short microtubules. Tubulins with MAPs were incubated with 10 μM paclitaxel (*A*), 100 μM vinblastine (*B*), or 100 μM A-105972 (*C*) in 30% glycerol containing 1 mM GTP for 30 min. Polymerization was initiated by the addition of tubulins. The samples were fixed, processed, and examined under EM at ×180,000.

Apoptosis and bcl-2 Phosphorylation Induced by A-105972. The effect of A-105972 on induction of apoptosis was also examined. Fig. 7*A* shows that A-105972 induced the formation of a DNA ladder in a dose- and time-dependent manner in HCT-15 cells. The effect of A-105972 on induction of apoptosis was observed after a 24-h incubation period. A concentration as low as 10 nM A-105972 was able to induce DNA fragmentation. The IC_{50} of A-105972 on inducing apoptosis is estimated to fall between 10 and 100 nM. It is important to note that HCT-15 cells are MDR+.

Fig. 7*B* shows that treatment of HT-1080 cells with 1 μM A-105972 for 24 h resulted in disruption of microtubules and formation of apoptotic bodies. These results suggest that A-105972 causes microtubule disruption and apoptosis in cancer cells.

Fig. 7*C* shows that in the MDR+ HCT-15 cells, treatment with 500 nM A-105972 for 24 h resulted in the phosphorylation of bcl-2, whereas 100 nM paclitaxel had no effect. The effect of A-105972 could be observed after 12 h of incubation. These results further confirm that A-105972 induces apoptosis, possibly via inactivation of bcl-2.

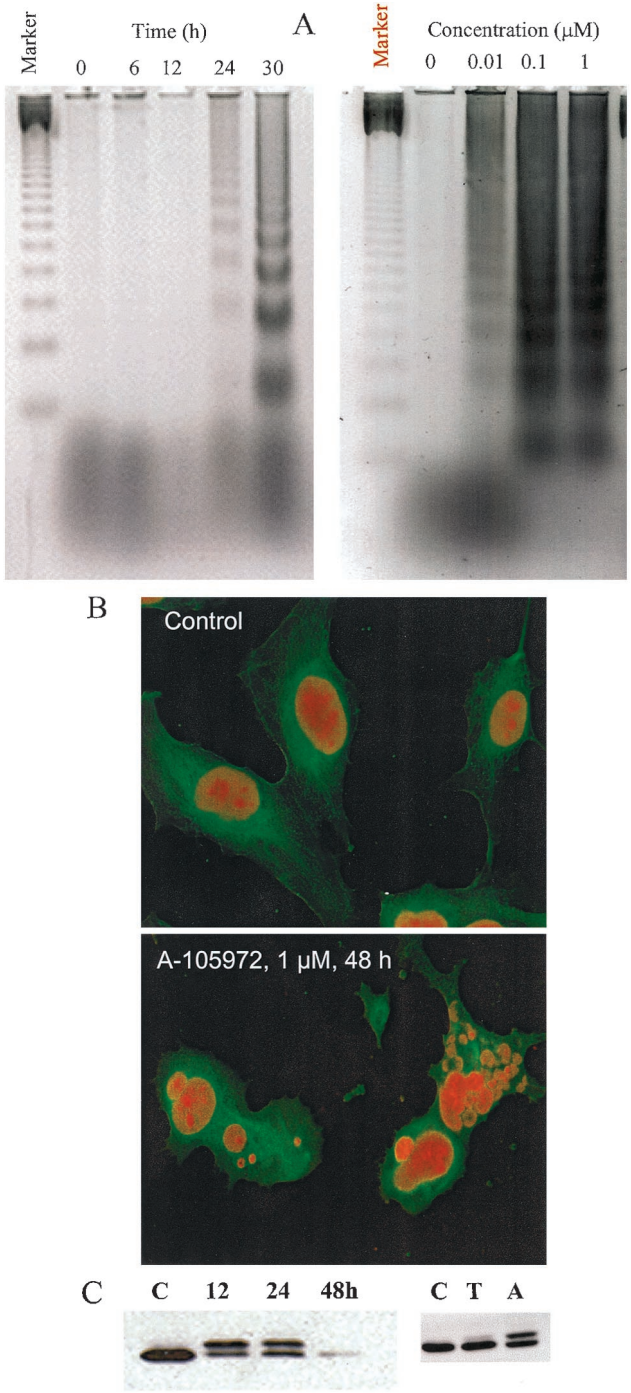

Fig. 7. A-105972 induced apoptosis and bcl-2 phosphorylation. *A*, DNA ladder. Total DNA was extracted from HCT-15 cells treated with 1 μM A-105972 for different periods of time (*left panel*) or treated with different concentrations of A-105972 for 24 h (*right panel*). DNA fragmentation was analyzed by electrophoresis as described in "Materials and Methods." *B*, confocal image. HT-1080 cells were treated with (*bottom panel*) or without (*top panel*) 1 μM A-105972 for 24 h. The cells were processed and stained for tubulin (*green*) and DNA (*red*) as described in "Materials and Methods." *C*, HCT-15 cells were treated with 1 μM A-105972 for different periods of time or with 100 nM paclitaxel (*T*) or 500 nM A-105972 (*A*) for 24 h. *C*, control, no addition of test agents. Cellular extracts were prepared and analyzed by SDS-PAGE and Western blotting as described in "Materials and Methods."

DISCUSSION

A-105972 was identified after screening >60,000 compounds in a high-throughput screening assay based on the inhibition of cell proliferation. A screening assay based on inhibition of cell growth offers the advantage of casting a wide net to potentially capture compounds working via many different mechanisms of action. The disadvantage of such a screening assay is that once a lead compound is identified, it is necessary to identify the specific mechanism of action to optimize the pharmacological and pharmacokinetic properties of the compound. In this study, we demonstrate that after A-105972 was identified as a lead compound from a cell proliferation-based screening assay, it was possible to quickly identify its mechanism of action.

Our data clearly show that A-105972 is efficacious in inhibiting the proliferation of various cancer cells. More importantly, the potency of A-105972 is completely independent of the levels of MDR, MRP, and LRP and is also independent of the status of the p53 protein. In addition to exhibiting potency in inhibiting cancer cell proliferation *in vitro*, A-105972 demonstrated efficacy in increasing the life span of mice inoculated with cancer cells. A-105972 yielded a half-life of less than 30 min in mice, thus hampering the *in vivo* efficacy evaluations. Our analytical chemical analysis indicated that the oxadiazolyl ring in A-105972 is not stable, and the compound may be slowly degraded into two components: trimethoxybenzaldehyde and a putative amide. Both components are inactive in inhibiting cell proliferation. The observation suggests that stabilizing the central ring of A-105972 will result in analogues with higher potency. After the mechanism of A-105972 was identified, we were able to design biochemical assays to test A-105972 analogues to develop compounds with improved stability and pharmacological and pharmacokinetic properties.

A-105972 disrupts microtubule assembly, as shown in the immunocytostaining and *in vitro* microtubule assembly studies. The *in vitro* tubulin polymerization study using the light scattering method shows that A-105972 at 100 μM completely blocked microtubule assembly when purified tubulin without MAPs was used. As a comparison, when MAP-rich tubulin was used, A-105972 at the same concentration only partially inhibited microtubule assembly. The impact of A-105972 on the rate of microtubule assembly from MAP-rich tubulin seems to be more evident in the initial phase of the polymerization. Interestingly, A-105972 treatment results in short microtubules when MAP-rich tubulin was used, as observed in the EM study. It has been shown that when tubulin polymerization occurs *in vitro* in the presence of assembly-inhibiting drugs, the dynamics of the microtubule polymers is disturbed. Some drugs may "cap" the net assembly end of the polymer while permitting disassembly to proceed uninhibited at the opposite end. A typical example of such an agent is colchicine (12). A-105972, as a tubulin-interacting compound, may also block microtubule assembly by capping the assembly end. Depending on the time and conditions in the *in vitro* tubulin polymerization assay, the results may be microtubules with substantially shorter length. Alternatively, A-105972 may block the elongation phase in microtubule assembly from the MAP-rich tubulin subunit, but it has no effect on the dynamics of the microtubule polymers, which may also result in the formation of shortened microtubules.

Results from biochemical studies clearly demonstrate that A-105972 binds to tubulin at a site distinct from vinblastine and paclitaxel. However, it is less clear whether the binding site of A-105972 is the same as or different from the colchicine binding site. Our competition studies show that colchicine is able to partially block [^{3}H]A-105972 binding to purified tubulin. The results suggest to us that the A-105972 binding site likely partially overlaps the colchicine binding site. However, the two sites may not be identical. It is perhaps of interest to add that when analogues of A-105972 were synthesized, some of them were shown to directly compete with [^{3}H]colchicine binding with K_i values in the low micromolar range,[3] whereas others were not efficacious in competing with [^{3}H]colchicine binding at all.

The mechanism of action of tubulin-interacting agents includes disruption of the microtubule assembly (vinblastine and colchicine) and stabilization of microtubules (paclitaxel). These agents are damaging to cells because they affect the dynamics of various microtubule-dependent cytoplasmic structures that are required for important cellular functions such as mitosis, maintenance of cellular morphology, vesicle transport, signal transduction, and so forth. Recently, tubulin-interacting compounds including paclitaxel and vinblastine have been shown to induce apoptosis by stimulating bcl-2 phosphorylation (13). In this report, we show that A-105972 is also able to induce bcl-2 phosphorylation and apoptosis. More importantly, A-105972 is capable of inducing apoptosis in MDR+ cancer cells.

The K_d value for the binding of A-105972 to purified tubulin is calculated to be 2.8 μM. It is evident that the potency of A-105972 in inhibiting cell proliferation (Fig. 1) and inducing apoptosis (Fig. 7) is at least 10–100-fold better than its binding affinity for tubulin. A similar observation was made for other tubulin-interacting compounds such as vinblastine and paclitaxel. The seeming discrepancy between the tubulin binding affinity and the cytotoxic efficacy of tubulin-interacting agents could be explained by the crucial role that microtubules play in maintaining normal cellular functions. Previously, Jordan *et al.* (14) and Margolis and Wilson (15) have shown that low concentrations of various microtubule assembly inhibitors sufficient to interfere with microtubule dynamics but not sufficient to disturb the morphology of the mitotic spindle can freeze mitotic cells at metaphase. Nevertheless, we could not exclude the possibility that A-105972 may affect molecular targets other than microtubules, resulting in the enhanced cytotoxicity.

In conclusion, we have shown in this report that A-105972, a synthetic small molecule identified from high-throughput screening, exhibits efficacy toward MDR+ cancer cells both *in vivo* and *in vitro*. A-105972 and its analogues are potentially useful in treating multidrug-resistant cancer.

REFERENCES

1. Ramachandran, C., and Melnick, S. J. Multidrug resistance in human tumors: molecular diagnosis and clinical significance. Mol. Diagn., *4:* 81–94, 1999.
2. Aran, J. M., Pastan, I., and Gottesman, M. M. Therapeutic strategies involving the multidrug resistance phenotype: the *MDR1* gene as target, chemoprotectant, and selectable marker in gene therapy. Adv. Pharmacol., *46:* 1–42, 1999.
3. Cole, S. P., and Deeley, R. G. Multidrug resistance mediated by the ATP-binding cassette transporter protein MRP. Bioessays, *20:* 931–940, 1998.
4. Scheffer, G. L., Wijngaard, P. L. J., Flens, M. J., Inzquierdo, M. A., Slovak, M. L., Pinedo, H. M., Meijer, C. J. L. M., Clevers, H. C., and Scheper, R. J. The drug resistance-related protein LRP is the human major vault protein. Nat. Med., *1:* 578–582, 1995.
5. O'Connor, P. M., Jackman, J., Bae, I., Myers, T. G., Fan, S., Mutoh, M., Scudiero, D. A., Monks, A., Sausville, E. A., Weinstein, J. N., Friend, S., Fornace, A. J., Jr., and Kohn, K. W. Characterization of the p53 tumor suppressor pathway in cell lines of the National Cancer Institute anticancer drug screen and correlations with the growth-inhibitory potency of 123 anticancer agents. Cancer Res., *57:* 4285–4300, 1997.
6. Dayton, B. D., Chiou, W. J., Opgenorth, T. J., and Wu-Wong, J. R. Direct determination of endothelin receptor antagonist levels in plasma using a scintillation proximity assay. Life Sci., *66:* 937–945, 2000.

[3] S. K. Tahir, E. K-H. Han, R. B. Credo, S. H. Rosenberg, H-S. Jae, J. A. Pietenpol, J. R. Wu-Wong, and S-C. Ng. A-204197, a novel oxadiazoline derivative with antimitotic activity in multidrug-sensitive and -resistant tumor cell lines, submitted for publication.

7. Shelanski, M. L., Gaskin, F., and Cantor, C. R. Microtubule assembly in the absence of added nucleotides. Proc. Natl. Acad. Sci. USA, *70:* 765–768, 1974.
8. Grever, M. R., Schepartz, S. A., and Chabner, B. A. The National Cancer Institute: Cancer Drug Discovery and Development Program. Semin. Oncol., *19:* 622–638, 1992.
9. Boyd, M. R., and Paull, K. D. Some practical considerations and applications of the National Cancer Institute *In Vitro* Anticancer Drug Discovery Screen. Drug Dev. Res., *34:* 91–109, 1995.
10. Wilson, L., and Jordan, M. A. Microtubule dynamics: taking aim at a moving target. Chem. Biol., *2:* 569–573, 1995.
11. Jordan, M. A., and Wilson, L. Microtubules and actin filaments: dynamic targets for cancer chemotherapy. Curr. Opin. Cell Biol., *10:* 123–130, 1998.
12. Margolis, R. L., and Wilson, L. Addition of colchicine-tubulin complex to microtubule ends: the mechanism of substoichiometric colchicine poisoning. Proc. Natl. Acad. Sci. USA, *74:* 3466–3470, 1977.
13. Wang, L. G., Liu, X. M., Kreis, W., and Budman, D. R. The effect of antimicrotubule agents on signal transduction pathways of apoptosis: a review. Cancer Chemother. Pharmacol., *44:* 355–361, 1999.
14. Jordan, M. A., Toso, R. J., Thrower, D., and Wilson, L. Mechanism of mitotic block and inhibition of cell proliferation by Taxol at low concentrations. Proc. Natl. Acad. Sci. USA, *90:* 9552–9556, 1993.
15. Margolis, R. L., and Wilson, L. Microtubule treadmilling: what goes around comes around. Bioessays, *20:* 830–836, 1998.